Advanced Nano Research
Volume 2, Issue 1, pp. 1-13, 2019
DOI: https://doi.org/10.21467/anr.2.1.1-13
ISSN: 2581-5164

RESEARCH ARTICLE

High Tunability of Size Dependent Optical Properties of ZnO@M@Au (M = SiO_2, In_2O_3, TiO_2) Core/Spacer/Shell Nanostructure

Gashaw Beyene Kassahun

Adama Science and Technology University, Adama, Ethiopia

* Corresponding author email: gashaw4nuclear@gmail.com

Received: 01 December 2018 / Accepted: 09 January 2019 / Published: 12 January 2019

ABSTRACT

This theoretical work presents a comparative study of high tunability size dependent optical properties of quantum dot/wire triple layered core shell nanostructure based on the quasi-static approximation of classical electrodynamics embedded in a fixed dielectrics function of host matrix. In this paper, local field enhancement factor (LFEF), refractive index and optical absorbance of nanocomposite are analyzed by varying core size, thickness of spacer and shell as well as dielectrics function of the spacer for the size of the nanocomposite with the range of 20 nm to 40 nm. For both quantum dot and quantum wire triple layered core shell nanostructure (CSNS), there are two resonances in visible and near/in infrared spectral region with high tunability. When the shell thickness increase and therefore increasing the gold content, the surface plasmon resonance (SPR) at the outer interface shifts to higher energy (blue-shifted) and at the inner interface weak peaks and shifted to lower energy (red-shifted). All of three optical properties, depend on core size, dielectrics and thickess of spacer, thickness of shell, shape of composite and filling factor. For the same thickness of spacer and shell of the two configurations, cylindrical triple layered CSNS less pronounced and shifted to infrared red (IR) spectral region which is recommendable for biological and photocatalysis application.

Keywords: Local field enhancement factor, Refractive index, Effective dielectrics, Filling factor, Host matrix, Optical absorbance

1 Introduction

Simply, core-shell or core-multishell is the system that involve two or more particles and/or compounds by using encapsulation process in different shape and size to obtain a final material with combined properties and other unique properties neither shown by the core nor by shell nanostructures due to the interaction of shell materials with the electromagnetic field which is greatly intensified by a phenomenon known as the surface plasmon resonance (SPR). Core shell nanoparticles (CSNPs) are nanostructured materials with interesting characteristics that offer a broad range of applications in optics, biomedicine [1], environmental science [2], materials chemistry [3], catalysis [4], information storage and energy because they have excellent properties such as versatility, tunability, and stability. They have attracted tremendous attention to their dramatically tunable plasmonic/optical properties. This unique property originates from the confined spatial distribution of the polarization charges over the surface of the nanostructure is taken as one of the main secrets of their application.

The uniformly coated shell on its core provides enhancement to the core along with passivation and extra functionalities. An appropriate shell layer modifies the properties of nanoparticles and simultaneously its application, can protect the core from the damage of high energy laser pulses, improve resistance to possible chemical reactions with its environment and even modify the properties of nanoparticles. Noble metal nanoparticles (NPs) are of great interest due to their special optical [5], electronic [5], and catalytic [5],[6] properties. In addition to their potential applications, noble metal nanoparticles are also of interest on account of the ability to tune their surface plasmon absorption band by changing their size. The plasmon

absorption band is a result of the interaction between the electric/electromagnetic field of light and the collective oscillation of the conduction electrons at the nanoparticles surface [7]. Among noble metal NPs, Au NPs have been investigated most extensively because of their facile preparation, resistance to oxidation, and surface plasmon resonance (SPR) band that can absorb and scatter visible light.

The interaction of plasmons with the surrounding medium and with the excites of the core materials leads to new optical features. For instance, energy and electron transfer from plasmon resonant metal surfaces to adjoining semiconductors can dramatically alter their optical properties, making semiconductor-metal nanocomposites a new class of multifunctional optical components, specially nanoparticles with a core shell configuration.

Triple layerd core shell nanostructure is studied either by experimentally or theoretically or by combining both by many researchers because of their new applications and unique physical and chemical feature. For instance, in [8], triple layered ZnO@Ag@ZnO explained by both experimentally and theoretically the effect of plasmon-exciton coupling on optical properties, in M. Liu et al [9], reported experimentally the influence of spacer, in the other paper [10], reported the biological application of triple layered CSNS. As explain in detail in [11], CSNS combine in different way, among these and triple layered CSNS, semiconductor-semiconductor-metal in one the most important combination. As far as my knowledge, triple layered metal Au coated materials are archetypal system for the study of exciton-exciton-plasmon interaction for optical and other applications with high tunability, is not studied yet.

Inspired by the above considerations, in this paper, noble metal Au NP as a shell, ZnO NP as a core and for spacer nanoparticles SiO2, In_2O_3 and TiO_2 are selected. These spacer materials have unique properties and used in large application field comparatively with the core material ZnO, for instance, SiO_2 has high chemical and thermal stabilities, catalysis, good compatibilities with other materials and chemical inertness, exhibited enhanced stability, optical and physical properties [12], In_2O_3 is an important n-type semiconductor with wide band gap of $3.55 - 3.75\ eV$, high optical transparency, high electrical conductivity and excellent luminescence, which holds potential applications in transparent electronics, light-emitting diodes, catalysis, solar cells , gas sensors and lithium-ion batteries [13],[14] and the third material titania (TiO_2) has desirable properties such as high corrosion-resistance, abundance, low price, non-toxicity and large band gap (3.2 eV) [15] and potential application in many fields [15], [16] mostly in photocatalysis [17]. These triple layered core shell NPs can be modified by varying the plasmon resonant frequency through varying the parameters like core size, the shape and size of nanocomposite, dielectrics of spacer and the interparticle distance. And by optimizing these parameters, the wavelength of the surface plasmon resonance shifted to the desired range, allowing for visible or infrared light absorption.

As explained in [2],[18],[19], ZnO nanoparticle has a potential application and unique optical properties than the other semiconductor materials. Recently, it was found that surface coating with different semiconductors and/or noble metal can dramatically change the properties of ZnO nano-crystallites as well as its applications [20].

In this work, I explained the effects of core size, thickness of spacer and shell, dielectrics function of the spacer, size and shape of nanocomposite on the local enhancement factor, refractive index and optical absorbance of the ZnO@M@Au triple layered core shell based on the quasi-static approximation. The applied electric field enhanced by the core material covered by noble metal when the frequency of incident and plasmon resonance frequency as well as applied field and inter atomic fields are comparative and it has many applications [21]. This composite demonstrated that a thin shell of noble metal Au surrounding a spherical nanodot and cylindrical nanowire semiconductor core and semiconductor (SiO_2, In_2O_3, TiO_2) spacer between ZnO and Au exhibits two surface plasmon resonances associated with the outer and inner surfaces of the shell. As the shell thickness is decreased the two surface plasmons will interact with each other more strongly and hence shift in position relative to the position of the individual resonances of the sphere surface or cavity occurs. A detailed theoretical and numerical analysis of the local field enhancement, refractive index and optical absorbance in small metal covered nanocomposite inclusions in the electrostatic approximation is the aim of this study. In section 2, I analyzed the distribution of electric potential in a

noble metal coated quantum dot/wire nanoparticle when incident electric field is applied to the composite and embedded into a fixed dielectric function of host matrix. Finally, in section 3, the results of numerical calculations are illustrated graphically. In the conclusion, I summarized the main results of the paper.

2 Theoretical Model and Calculation

As was shown in several works, the overall optical as well as plasmonic properties of triple and two layered nanoparticle successfully described within the framework of classical electrodynamics of continuous media. Similarly, for triple layered core shell of this work, I used the same consideration. In this paper, I seek to investigate highly tunable size dependent optical properties of spherical and cylindrical triple layered CSNS by varying the core size, thickness of spacer and shell and size/shape of composite as well well as dielectrics function of spacer.

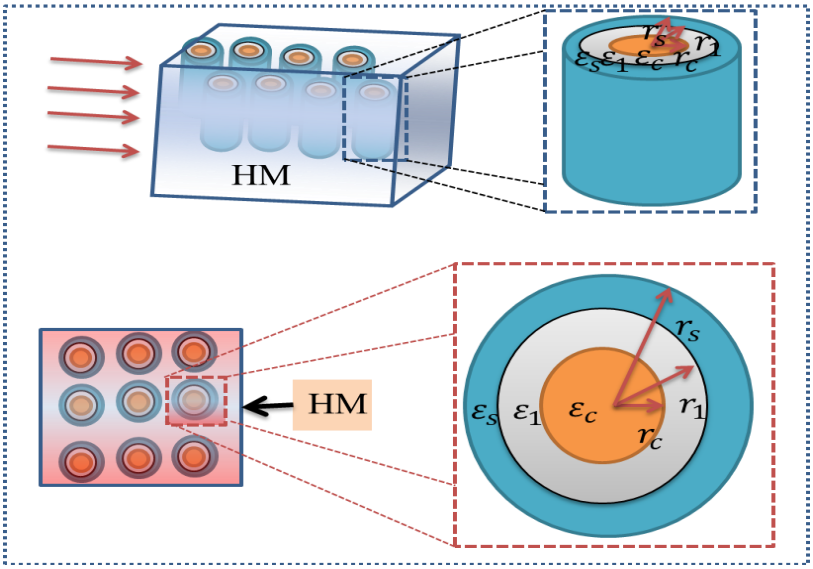

Figure 1: *The model of quantum dot/wire core/spacer/shell nanostructure: embedded in host matrix, quantum wire (top) and quantum dot (bottom) in applied electric field.*

Consider this triple layered core shell nanoparticle (NP) consisting of a semiconductor core of dielectric function (DF) ε_c , spacer ε_1 and a metallic shell of DF ε_s embedded in a non-absorptive host matrix having a real DF $\varepsilon_h = 2.25$, as shown in Fig. (1), i.e.; cross - sectional view of the composite. When the composite of triple layered CSNP is irradiated with an electromagnetic radiation, electric field is induced in the system due to polarization. The distribution of the electrostatic potential ϕ associated with the induced field inside and outside of the NP can be obtained by solving the Laplace equation, $\nabla^2\phi = 0$ in spherical and cylindrical coordinates.

The distribution of the potential in the four regions takes the form:

$$\phi_1 = A_1 r\cos\theta \qquad r \le r_c \qquad (1)$$

$$\phi_2 = \left(A_2 r + \frac{B_1}{r^{n-1}}\right)\cos\theta \qquad r_c \le r \le r_1 \qquad (2)$$

$$\phi_3 = \left(A_3 r + \frac{B_2}{r^{n-1}}\right)\cos\theta \qquad r_1 \le r \le r_s \qquad (3)$$

$$\phi_4 = \left(-E_0 r + \frac{B_3}{r^{n-1}}\right)\cos\theta \qquad r \ge r_s \qquad (4)$$

where ϕ_1, ϕ_2, ϕ_3 and ϕ_4 are the potentials in the core, semiconductor spacer, metal shell, and host matrix, respectively, E_0 is associated with the external applied field; r is the distance from the origin (centre of the NP); and θ is the zenith angle, r_c, r_1, and r_s are the radius of the core, the spacer and the metal shell, respectively. And here, n is the dimension of the problem: $n = 3$ for the spherical and $n = 2$ for the cylindrical inclusion, respectively and the coefficients A_1, A_2, A_3, B_1, B_2, B_3 are constants to be determined by using the appropriate boundary conditions at the interface.

It is worth noting that the second term on the right side of Eq. (4), represents the induced potential outside the composite NP. To study local filed enhancement factor, refractive index and optical absorbance, I need to determine only the total induced field outside the concentric sphere/cylinder and the coefficient of potential inside the core. In other words, I am interested on the value of the coefficients A_1 and B_3 rather

than other coefficients, which is found to be by concurrently using the above four equations based on normal component of the electric displacement vector and continuity condition of potential at the interfaces,

$$A_1 = -\frac{n^3}{n-1}\frac{\varepsilon_h\varepsilon_1\varepsilon_s}{\beta_2 X}E_0, \quad (5)$$

$$B_3 = {r_s}^n E_0\left(1 - \frac{n^3}{n-1}\frac{\varepsilon_h\left({}^{B}/_{\beta_2}+A\right)}{X}\right), \quad (6)$$

where

$$A = n{\varepsilon_1}^2 + \varepsilon_1(\varepsilon_c - \varepsilon_1)\left(\frac{n}{n-1}\right)\beta_1 - n\varepsilon_c\varepsilon_s - \varepsilon_s(\varepsilon_c - \varepsilon_1)\,\beta_1, \quad (7)$$

$$B = n^2\varepsilon_1\varepsilon_s + n\varepsilon_s(\varepsilon_c - \varepsilon_1)\,\beta_1, \quad (8)$$

$$X = C_1{\varepsilon_s}^2 + C_2\varepsilon_s + C_3, \quad (9)$$

$$\beta_1 = 1 - \left({}^{r_c}/_{r_1}\right)^n, \qquad \beta_2 = 1 - \left({}^{r_1}/_{r_s}\right)^n, \quad (10)$$

where β_1 and β_2 are the volume fraction of spacer and shell respectively and C_1, C_2 and C_3 are constants depend on dielectrics function of core, spacer and host matrix.

By substituting Eq (5) into Eq (1), we get the electric field inside the core material:

$$\phi_1 = -\frac{n^3}{n-1}\frac{\varepsilon_h\varepsilon_1\varepsilon_s}{\beta_2 X}E_0 r\cos\theta., \quad (11)$$

Then, using Eq. (11) and the relation $E = -\nabla\phi$, we find the magnitude of the electric field inside the core to be,

$$E = \frac{n^3}{n-1}\frac{\varepsilon_h\varepsilon_1\varepsilon_s}{\beta_2 X}E_0. \quad (12)$$

The coefficient of E_0 in Eq. (12) is the local-field enhancement factor (F), i.e.,

$$F = \frac{E}{E_0} = \frac{n^3}{n-1}\frac{\varepsilon_h\varepsilon_1\varepsilon_s}{\beta_2 X}. \quad (13)$$

The modulus square of the local field enhancement factor becomes

$$|F|^2 = \left|\frac{n^3}{n-1}\frac{\varepsilon_h\varepsilon_1\varepsilon_s}{\beta_2 X}\right|^2. \quad (14)$$

The induced potential outside the inclusion is,

$$\phi_{ind} = \frac{B_3}{{r_s}^n}\cos\theta. \quad (15)$$

The induced potential may be expressed by

$$\phi_{ind} = \frac{\tilde{p}}{4\pi\varepsilon_h{r_s}^n}\cos\theta, \quad (16)$$

where $\tilde{p}$ is the electric dipole moment of the system.

In a uniform external electric field, a dielectric object becomes polarized. In far field, the polarized object can be approximated as an electric dipole because the higher order field components decay quickly as a function of distance [22].

The electric dipole moment by combining the above equations:

$$\tilde{p} = 4\pi\varepsilon_h B_3 = \varepsilon_h\alpha E_0 \quad (17)$$

where α is the polarizability of the composite given by

$$\alpha = 4\pi{r_s}^n\left[1 - \frac{n}{n-1}\frac{\varepsilon_h({}^{B}/_{\beta_1}+A)}{X}\right]. \quad (18)$$

The polarizability and the effective permittivity of the system can be described by using the Clausius-Mossotti relation together with the Maxwell-Garnet mixing theory. Suppose N is the density numbers the inclusions/scatterers in the system. Then, the polarizability and permittivity are related by [23],

$$\frac{N\alpha}{3} = \frac{\varepsilon_{eff}-\varepsilon_h}{\varepsilon_{eff}+2\varepsilon_h}, \quad (19)$$

where ε_{eff} is the effective DF of the system (ensemble).

By rearranging the above Eq. (19), the ε_{eff} written as:

$$\varepsilon_{eff} = \varepsilon_h \left[1 + \frac{3f\alpha}{1-f\alpha}\right], \quad 20$$

known as Maxwell-Garnett equation and where f is the filling factor which tell us how much the array of composite embedded in the host matrix

$$f = {4\pi N r_s^n}/{3}. \quad 21$$

Some of the metal properties, including optical properties can be described with the simple free-electron gas Drude-Sommerfeld model of dielectric function. In the framework of this model, by applying an external field, the conduction electrons move freely between independent collisions occurring at the average rate of the frequency-dependent dielectric function $\varepsilon(\omega)$ predicted by the Drude-Sommerfeld model [24]:

$$\varepsilon(\omega) = \varepsilon_\infty - \frac{{\omega_p}^2}{\omega(\omega + i\,\gamma)}, \quad 22$$

where ε_∞ is the phenomenological parameter describing the contribution of bound electrons to polarizability, ω_p is the bulk plasmon frequency and γ is the phenomenological electron damping constant of the bulk material. For Au, $\varepsilon_\infty = 9.84$ and $\omega_p = 9.01\ eV$ [25].

The dimensional dependence of the dielectric function was introduced within the framework of the model of limitation of the mean free path of conduction electrons. Decreasing the size of a nanoparticle will eventually cause the thickness to become less than the bulk mean free path, and electron scattering from the surfaces of the particle will have decreasing effect thus broadening its plasmon resonance peaks. If the electron mean free path depends on size of the nanoparticles, a correction is available for the nanoshells and in this case, γ can be modified to [26],[27],[28]:

$$\gamma = \gamma_{bulk} + A\frac{v_F}{r_{eff}}, \quad 23$$

where $\gamma_{bulk} = 0.072\ eV$ [25] is the damping constant of the bulk material, $v_F = 1.38\ Mm/s$ [28] is the electron velocity at the Fermi surface, $A = 0.25$ is an empirical parameter and r_{eff} is the effective mean free path of collisions and can be calculated from [28],

$$r_{eff} = \left(\frac{((r_s - r_1)({r_s}^2 - {r_1}^2))^{1/3}}{2}\right). \quad 24$$

3 Results and Discussion

3.1 Local Field Enhancement Factor

The highly tunable optical properties and plasmon resonances of triple layered core shell making them attractive and may be considered by combining various types of materials, metals and semiconductors, where one material is a core, another different material is a spacer and shell.

The local field enhancement factor of ZnO@M@Ag spherical and cylindrical triple layered core shell that composed of 12 *nm* ZnO core radius, 16 nm spacer radius with different shell thickness nanoinclusion as a function of wavelength is depicted in Fg. (2). It is observed that, local field enhancement factor of gold coated two geometrical nanoinclusion is increase with increasing shell thickness. The two resonance at visible region and near/in infrared spectral region is related to the surface resonance of Au at the two interfaces i.e.; spacer@Au and Au@medium [29].

As shown in the figure (2), the resonance at wavelength around 460 nm associated with inner interface is remain constant, but the resonance associated with outer interface extends from visible to near infrared spectral region that is by controlling the resonance frequency via the shell thickness increase [30]. The thickness of Au shell increase from $4\ nm$ to $24\ nm$ correspondingly its volume fraction is 0.49, 0.70, 0.81, 0.86, 0.91 and 0.94 for a fixed spacer volume fraction 0.58 for spherical and for cylindrical composite 0.36, 0.56, 0.67, 0.75, 0.80, and 0.84 for spacer volume fraction 0.44. The local field enhancement factor for spherical inclusion Fig 2(A) for both resonances in visible spectral region more pronounced than the cylindrical inclusion Fig. 2(B). As Fig 2(B) illustrated, by varying the relative dimension of nanoinclusion,

the optical resonance of the composite varied, across visible region to infrared (IR) spectral region. In the other case, when the spacer material is changed the local field enhancement factor also changed, i.e.; when the dielectrics function of the spacer increased from Fig 2(C) to Fig. 2(D), the local filed enhancement factor increase within the same resonance peak location.

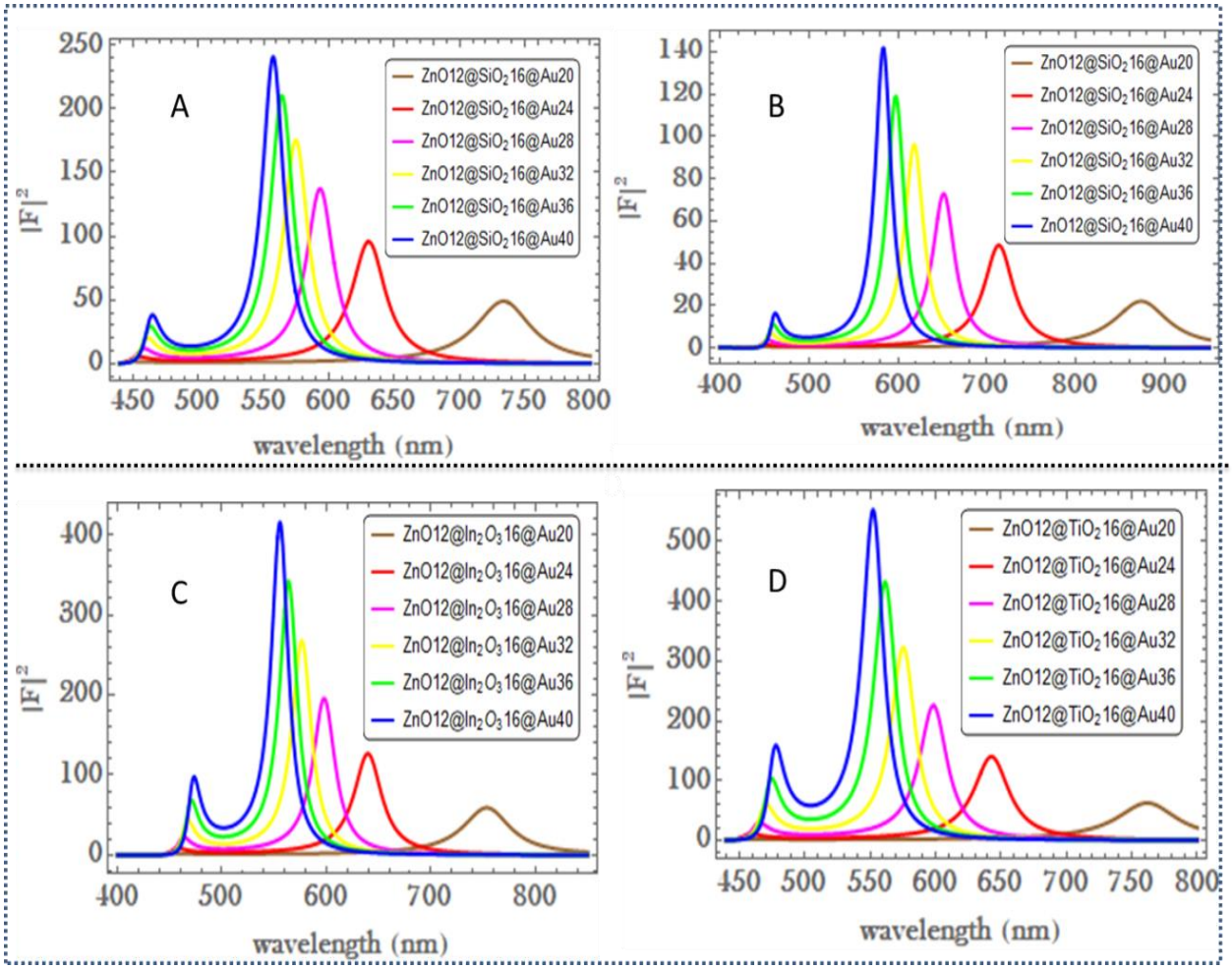

Figure 2: *Local filed enhancement factor with different geometry and spacer materials for increasing shell thickness. (A), (C), (D) spherical and (B) cylindrical triple layered nanoinclusion.*

The local filed enhancement factor of ZnO@M@Au is also depending on the concentration of the core and spacer materials. By increasing the core size and spacer thickness and by keeping the size of the composite constant $40\ nm$, the effect is explained in Fig (3). Either the core size or the spacer thickness increase simultaneously the shell thickness decrease from $24\ nm$ to $4\ nm$. As shown in the figure for spherical nanoinclusion, when the core size and spacer thickness increase, the local field enhancement factor decrease and extend to IR spectral region and has the same effect for cylindrical inclusion.

The concentration of spacer and metallic shell when the core size increase from $12\ nm$ to $32\ nm$ is 0.58, 0.49, 0.42, 0.37, 0.33, 0.30 and 0.94, 0.86, 0.78, 0.66, 0.49, 0.27 respectively. And similarly, for a fixed core size $12\ nm$, the concentration of spcer for Fig. 3(B) increase correspondingly 0.58, 0.78, 0.88, 0.92, 0.95, and 0.96. From this graph, we observed that the amplitude of local filed enhancement factor is slightly the same but there is high tunability in Fig. 3(A) due to high interaction of plasmon and exciton.

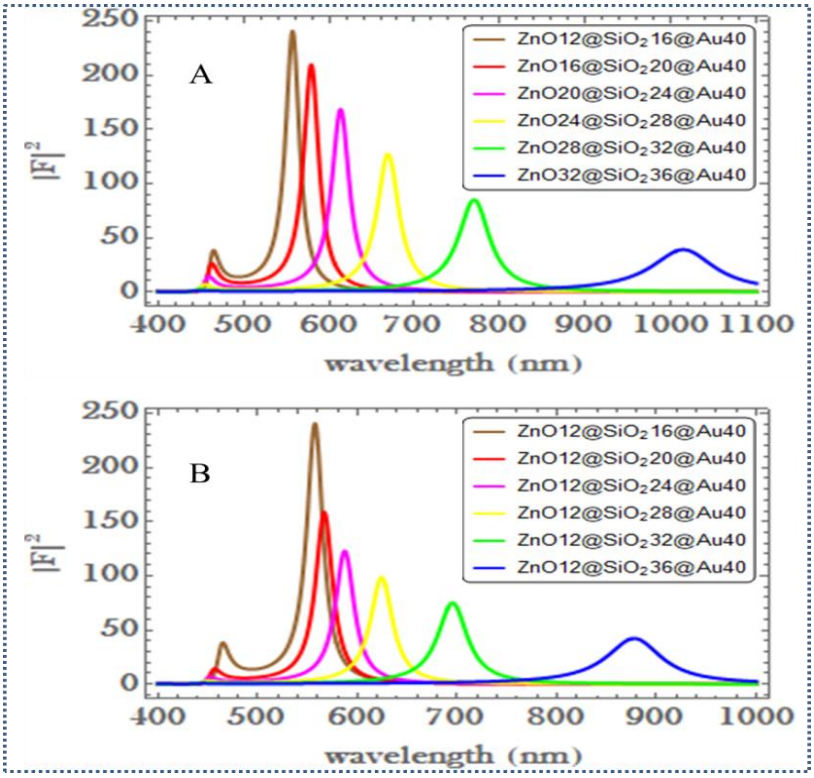

Figure 3: *Local filed enhancement factor with the same size of composite for decreasing shell thickness and increasing spacer volume fraction. (A) increase core size and (B) increase spacer thickness of spherical triple layered nanoinclusion.*

3.2 Refractive Index

Optical properties of matter are consquences of how it reflect, transmit and absorb in coming light. In many optical problems, the complex refractive index of material is the basic parameter. The refractive index of the medium related to its dielectrics function which describes the electronic interaction of the medium with incident light wave of frequency. The response of a medium to an incident light wave may be described by a complex refractive index $(\tilde{n})$ which for a nonmagnetic medium is expressed as

$$\tilde{n} = \sqrt{\varepsilon_{eff}} \qquad 25$$

where ε_{eff} is the complex effective DF of the composite. Introducing the real (n) and imaginary parts (k), $\tilde{n}$ may be written as [25]

$$\tilde{n} = n + i\,k \qquad 26$$

The real part of refractive index of an ensemble consisting ZnO@M@Au spherical and cylindrical core shell embedded in host matrix which have dielectric function $\varepsilon_h = 2.25$ is analysed using Eq. (25) and (26). Figure (4) shows the real part of refractive index as a function of wavelength of the incident light for a fixed value of the filling factor $f = 0.01$ and $\beta_1 = 0.58$ and six different values of β_2 ($\beta_2 =$ 0.49, 0.70, 0.81, 0.86, 0.91, 0.94). The grph shows that the refractive index varies between 1.30 and 1.71 depends on the geometry, size and constituents of the ensemble and posses two sets of resonance associate with the interface of the metal shell; the first resonance in visible region around $450\ nm$ and the second extended to IR region between $550\ nm$ and $1000\ nm$. The peaks show a slight red shift in the first resonance and blue shift in second resonance when the volume fraction, β_2 is increased.

In addition, when metal shell thickness increases the two resonance peaks gets closer and closer to each other which eventually merge if $\beta_2 = 1$. For the same size of the composite, simply by increasing the dilectrics function of the spacer, the refractive index of the composite more pronounced coresspondingly i.e.; the transmission of the incident ray is increase.

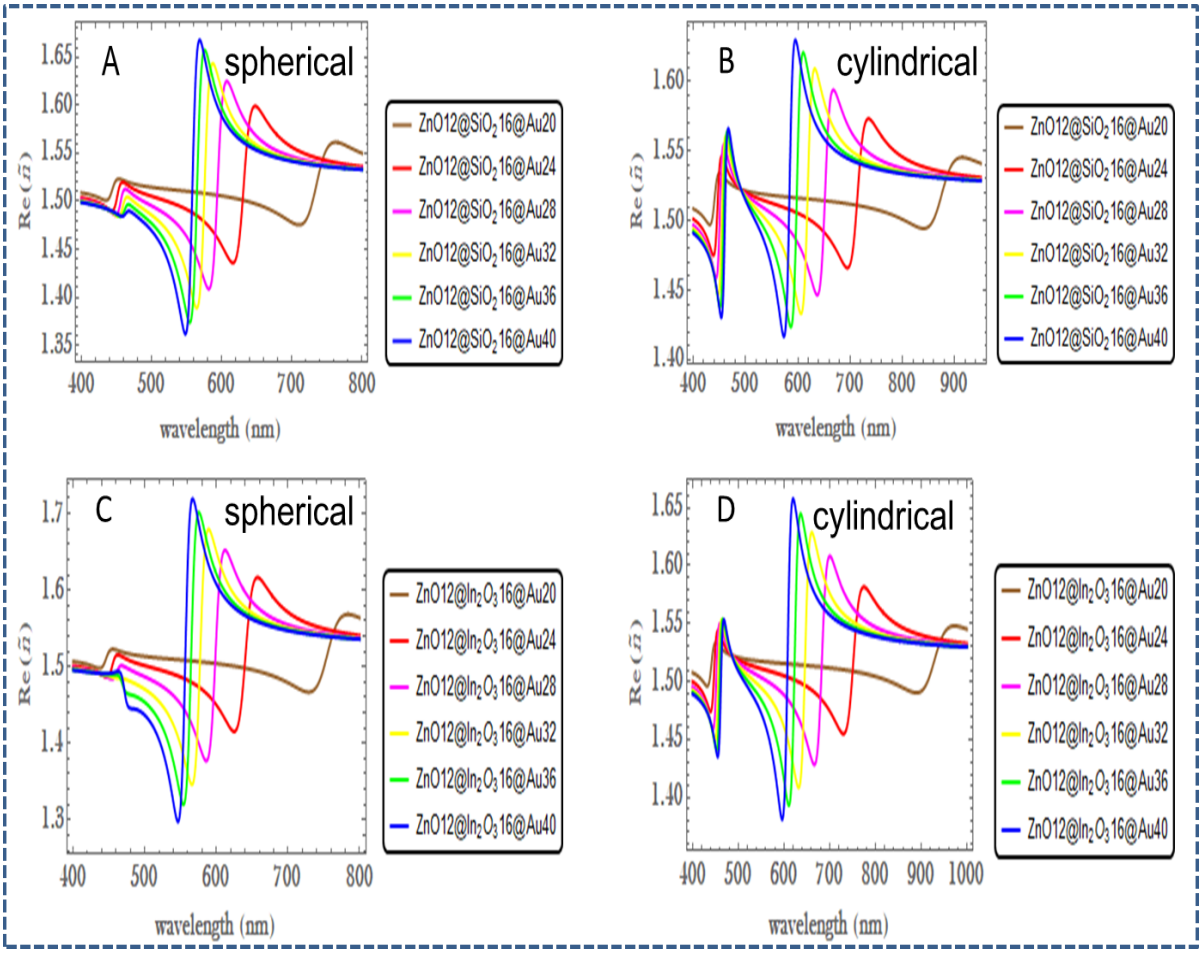

Figure 4: *The real part of refractive index as a function of wavelength for fixed filling factor $f = 0.01$, different Au volume fraction and by keeping spacer volume fraction constant. A and C spherical and B and D cylindrical are nonainclusion with different spacer.*

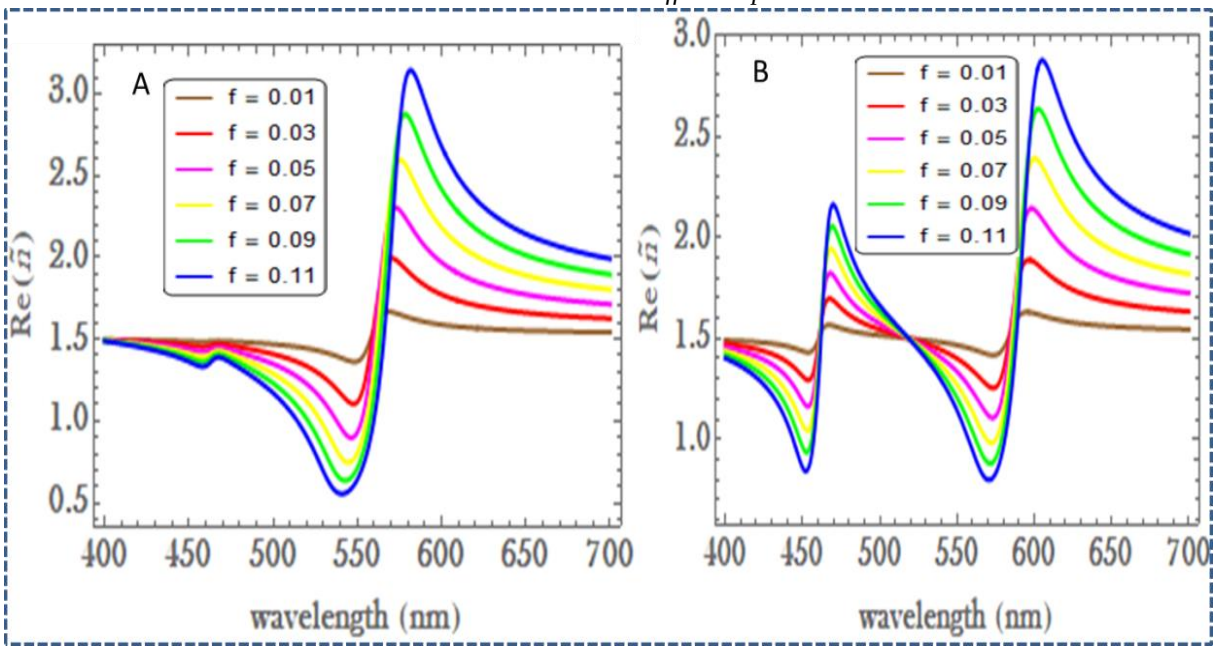

Figure 5: *The real part of refractive index as a function of wavelength for different value of filling factor f. A spherical and B cylindrical nanoinclusion. The other parameters are the same with Fig 4(A) and 4(B).*

Furthermore, I analyzed the effect of varying the filling factor, f, on the real part of refractive index in the vicinity of the two resonances progressively increases as f increases from 0.01 to 0.11 in step of 0.02 as shown in Figure 5. However, the positions of the peaks remains almost constant. The result suggests that light propagates in the nanostructure more readily when the nanoinclusion array is more packed. From both figures, refractive index near the resonances can be tuned by changing the shell thickness, dielectrics function of the spacer and the density of the packed arrays which can play a great role in applying the CSNS in the sensors.

3.3 Optical Absorbance

Incident light, in general, propagating in the composite is attenuated both by absorption and by scattering [31]. However, for NPs that are much smaller than the wavelength of incident light, scattering effects may be neglected so that only the absorption significant to the attenuation. The intensity (I) of the propagating wave is related to the enhanced electric field by $I\sim|E|^2$. Generally, as the wave traverses in the composite/medium, the intensity is attenuated as:

$$I_t = I_o \exp(-\mu t), \tag{27}$$

where I_o is the intensity at $t = 0$ and μ is the absorption coefficient defined by

$$\mu = \frac{2k\omega}{c} = \frac{4\pi k}{\lambda}, \tag{28}$$

where $\omega = 2\pi c/\lambda$ is the wavelength of the incident radiation and k is the imaginary part of the refractive index.

The quantity in the exponent of Eq. (27) is the absorbance (A) which may be generally be expressed as $A = \ln\left(\frac{I_o}{I_t}\right) = \mu t$ where I_t is the intensity at $t = t_{Au}$. For the ZnO@M@Au triple layered core shell NPs, the absorbance at metal/shell interface takes the form [32]:

$$A(\lambda) = \frac{4\pi k}{\lambda} t_{Au}, \tag{29}$$

where $t_{Au} = r_s - r_1$ thickness of gold shell.

Figure (6), depicts optical absorption of triple layered CSNS as a function of wavelength for $f = 0.01$ and $\beta_1 = 0.56$ and different value of β_2 (or different value of shell thickness), while the core and spacer radius (12 nm and 16 nm respectively) is kept constant. The metal shell volume fraction is increase with increasing shell thickness, correspondingly the value of β_2 are 0.49, 0.70, 0.81, 0.88, 0.91, and 0.94. It shows the two sets of absorption peaks: for spherical inclusion both absorption peaks are in visible region but for cylindrical inclusion extends to infrared region and shifted to visible region when the shell thickness increase.

As the shell thickness increase from $t_{Au} = 4 - 24\ nm$ with the range $4\ nm$, the first resonance rapdly enhanced and slightly red shifted, but for spherical inclusion slightly enhanced when the shell thickness increase. These resonances may be attributed to near band edge absorption (NBA) due to free exciton recombination. In these resonances, the red-shift of the absorption edge represented the change in the nanoparticles energy gap. It means that since the band gap of semiconductor materials will increase with the decrease in particle size, the so-called quantum size effect, it leads to the shift of the absorption edge towards high energy (blue-shift) [33].

The second resonances are also enhanced when the shell thickness is increase, but blue-shifted contrary to the first resonance. These resonance peaks are due to deep level emissions (DLE) which are attributed to the surface plasmon resonance of gold nanoshell. The absorption intensity become stronger as the thickness of gold shell increase from $4 - 24\ nm$. On the other hand, red shift of the absorption maximum with an increase in shell thickness and the broadening of the absorption spectra are observed when the thickness of the shell decrease [31]. This broadening of the spectra is caused because of the incorporation of the NPs size effect in our analysis via Eq (23).

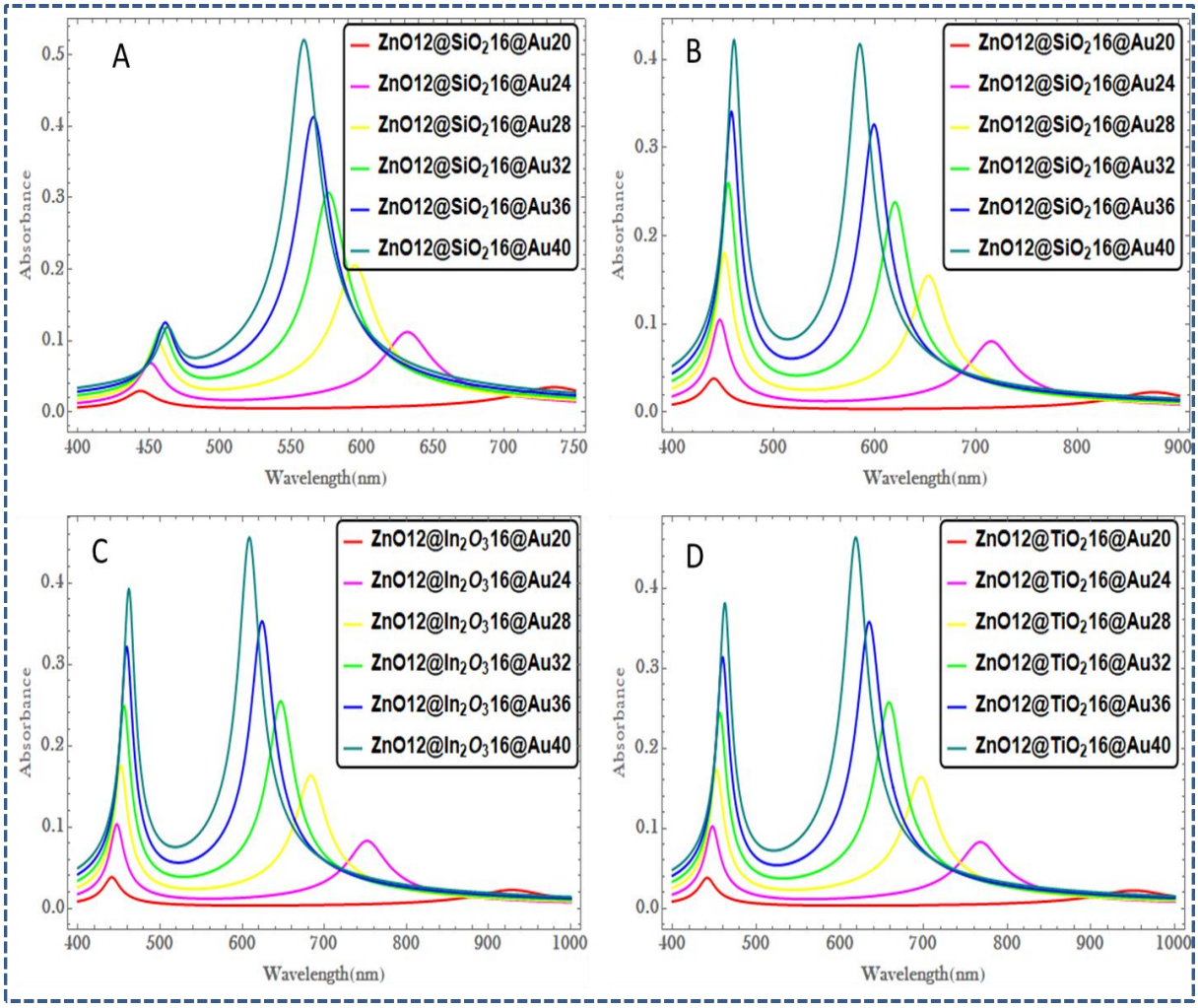

Figure 6: *Optical absorbance as a function of wavelength for different spacer materials. (A) spherical and the others are cylindrical nanoinclusion. The other parameters are the same with Fig 4.*

The optical absorbance of triple layered core shell not only depends on size and shape of the composite, it also depends on the size of the core and the thickness of spacer. When the thickness of spacer increase by keeping the core size $12\ nm$ and the shell thickness $4\ nm$ constant for spherical nanocomposite in figure 7(A), the optical absorbance in the second resonance which is associated with outer interface, decrease and shifted to higher wavelength IR spectral region. But in the first resonance around $450\ nm$ wavelength of this figure, the optical resonance slightly decrease and without shifting. The resonance peak for a single ZnO and Au nanoparticle is exist at visible region [34], but by combining them and by sandwiching other materials between them for the same size, the absorbance is enhanced and shifted to IR region that is interested phenomena for biological and photocatalysis application.

For cylindrical inclusion in Fig. 7(B), the optical absorbance is decrease with increasing core size by keeping spacer thickness $4\ nm$ and composite size $40\ nm$ constant i.e.; the thickness of shell decrease with increasing core size. The first resonances are rapidly decreased with slightly blue-shift, but in the second resonance slowly decrease relative to the first resonance and shifted to higher wavelength in IR spectral region. This high tunability arises from the interaction of cavity plasmon in the plasmon hybridization associated with inner and outer interfaces [5]. The hybridization interaction is stronger for thinner shell layer, leading to a strongly red-shifted resonance at a wavelength determined by the thickness of the shell and the overall particle radius.

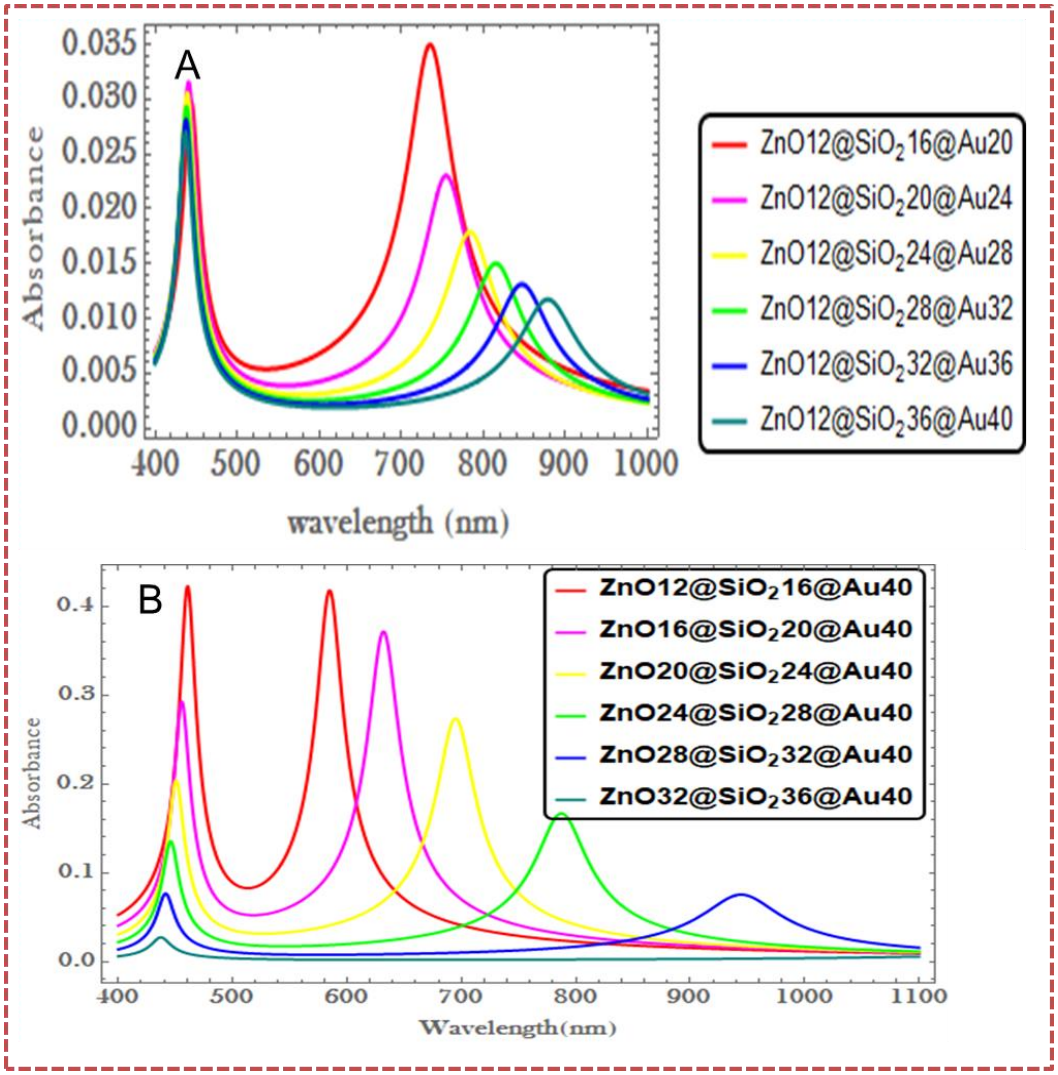

Figure 7: *Optical absorbance as a function of wavelength (A) increasing spacer volume fraction and (B) increasing core size. (A) spherical and (B) cylindrical nanoinclusion.*
The other parameters are the same with Fig 4.

4 Conclusions

The results obtained for spherical and cylindrical triple layered core shell nanoparticle consists of ZnO as core, semiconductor spacer (like SiO_2, In_2O_3, TiO_2) and a noble metal Au as a shell with dimension much less than the wavelength of light using the quasi-static approximation of classical electrodynamics embedded in a fixed deilectrics function ($\varepsilon_h = 2.25$) of the host matrix. The local filed enhancement factor, refractive index, and optical absorbance of the system are determined by employing the electrostatic potential approximation and the Maxwell-Garnet effective medium theory. Moreover, the DF of the gold shell is chosen to be of the modified Drude form that takes into account its nano-size scale.

It is shown that for different values of spacer and metal shell fraction, dielectrics function of spacer, core size, size of nanoinclusion and filling factors f the graphs of local field enhancement factor, optical absorbance and refractive index of the nanocomposite with ZnO@M@Ag nanoinclusions as a function of wavelength possess two resonance peaks - the first in the visible region (around 450 *nm*) and the second extends from visible to IR (between 550 - 1100 *nm*) spectral regions. These resonance peaks correspond to the surface plasmon resonances at the inner and outer interfaces, respectively. The resonance peaks show a slight red shift in the first resonances and blue shift in the second resonances when the volume fraction of shell thickness increased. The optical resonance prounounced when the dielectrics of the spacer

increased, shape of composite changed and the filling factor increased. Due to the interaction beteween environment and plasmon of shell, exciton and plosmon, the amplitude of plasmon resonances increased when the cylidrrical nanoinclusion changed to spherical inclusion and the filling factor increased. Inddition, by increasing dielectrics function of spacer and for cylindrical inclusion the optical resonance is more tuned. Such types of highly tunability of optcal properties is recommended for many application fields like biological, photocatlytic, energy storage, information storage and sensor. The enhancement in the optical properties is mainly attributed to strong coupling of the surface plasmon resonance of the Au shell and the energy gap of the inner part NPs, interaction of exciton-excion-plasmon of the composite, and interaction of the composite with it envirnment.

5 Acknowledgments

This work was supported financially by Adama Science and Technology University (ASTU), Adama, Ethiopia.

How to Cite this Article:

G. Kassahun, "High Tunability of Size Dependent Optical Properties of ZnO@M@Au (M = SiO_2, In_2O_3, TiO_2) Core/Spacer/Shell Nanostructure", *Adv. Nan. Res.*, vol. 2, no. 1, pp. 1-13, Jan. 2019. Doi: 10.21467/anr.2.1.1-13

References

[1] Y. Wu and P. Nordlander, "Plasmon hybridization in nanoshells with a nonconcentric core," *J. Chem. Phys.*, vol. 125, no. 12, 2006.
[2] X. Shao, B. Li, B. Zhang, L. Shao, and Y. Wu, "Au@ZnO core-shell nanostructures with plasmon-induced visible-light photocatalytic and photoelectrochemical properties," *Inorg. Chem. Front.*, vol. 3, no. 7, pp. 934–943, 2016.
[3] M. B. Gawande *et al.*, "Core-shell nanoparticles: synthesis and applications in catalysis and electrocatalysis," *Chem. Soc. Rev.*, vol. 44, no. 21, pp. 7540–7590, 2015.
[4] B. K. Ghosh and N. N. Ghosh, "Applications of Metal Nanoparticles as Catalysts in Cleaning Dyes Containing Industrial Effluents: A Review," *J. Nanosci. Nanotechnol.*, vol. 18, no. 6, pp. 3735–3758, 2018.
[5] B. E. Brinson, J. B. Lassiter, C. S. Levin, R. Bardhan, N. Mirin, and N. J. Halas, "Nanoshells made easy: Improving Au layer growth on nanoparticle surfaces," *Langmuir*, vol. 24, no. 24, pp. 14166–14171, 2008.
[6] P. K. Jain, K. S. Lee, I. H. El-sayed, and M. A. El-sayed, "Calculated Absorption and Scattering Properties of Gold Nanoparticles of Different Size, Shape, and Composition: Applications in Biological Imaging and Biomedicine," *J. Phys. Chem. B*, vol. 110, no. 14, pp. 7238–7248, 2006.
[7] S. Zahra and H. Minabi, "The effect of temperature on optical absorption cross section of bimetallic core-shell nano particles," vol. 1, no. 3, 2016.
[8] M. E. Koleva, N. N. Nedyalkov, and P. A. Atanasov, "Effect of the plasmon-exciton coupling on the optical response of a ZnO/Ag/ZnO nanocomposite," *J. Phys. Conf. Ser.*, vol. 514, no. 1, pp. 8–12, 2014.
[9] M. Liu *et al.*, "Tuning the influence of metal nanoparticles on ZnO photoluminescence by atomic-layer-deposited dielectric spacer," *Nanophotonics*, vol. 2, no. 2, pp. 153–160, 2013.
[10] H. Chen *et al.*, "CHARACTERIZATIONS AND ANTIBACTERIAL PROPERTIES OF ZnS / ZnO CORE-SHELL STRUCTURES ON SILVER WIRES," *J. Optoelectron. Biomed. Mater.*, vol. 9, no. 4, pp. 171–178, 2017.
[11] N. Senthilkumar, M. Ganapathy, A. Arulraj, M. Meena, M. Vimalan, and I. Vetha Potheher, "Two step synthesis of ZnO/Ag and ZnO/Au core/shell nanocomposites: Structural, optical and electrical property analysis," *J. Alloys Compd.*, vol. 750, pp. 171–181, 2018.
[12] M. A. Salim, H. Misran, S. Z. Othman, N. Mahadi, N. I. M. Pauzi, and A. Manap, "Synthesis and Characterizations of SiO2-Ag Core-Shell Nanostructure Using Fatty Alcohols as Surface Modifiers," *Appl. Mech. Mater.*, vol. 773–774, no. November, pp. 199–203, 2015.
[13] L. Yue *et al.*, "One-step solvothermal process of In2O3/C nanosheet composite with double phases as high-performance lithium-ion battery anode," *Electrochim. Acta*, vol. 160, pp. 123–130, 2015.
[14] A. Qurashi, M. F. Irfan, and M. W. Alam, "In2O3 nanostructures and their chemical and biosensor applications," *Arab. J. Sci. Eng.*, vol. 35, no. 1 C, pp. 125–145, 2010.
[15] A. Müller *et al.*, "Morphology, Optical Properties and Photocatalytic Activity of Photo- and Plasma-Deposited Au and Au/Ag Core/Shell Nanoparticles on Titania Layers," *nanomaterials*, vol. 502, no. 8, pp. 6–12, 2018.
[16] B. Bartosewicz, M. Michalska-Domanska, M. Liszewska, D. Zasada, and B. J. Jankiewicz, "Synthesis and characterization of noble metal-titania core-shell nanostructures with tunable shell thickness," *Beilstein J. Nanotechnol.*, vol. 8, no. 1, pp. 2083–2093, 2017.
[17] Y. Lin *et al.*, "The optical absorption and hydrogen production by water splitting of (Si,Fe)-codoped anatase TiO2photocatalyst," *Int. J. Hydrogen Energy*, vol. 38, no. 13, pp. 5209–5214, 2013.
[18] E. J. Guidelli, O. Baffa, and D. R. Clarke, "Enhanced UV Emission from Silver/ZnO and Gold/ZnO Core-Shell Nanoparticles: Photoluminescence, Radioluminescence, and Optically Stimulated Luminescence," *Sci. Rep.*, vol. 5, no. August, pp. 1–11, 2015.
[19] A. Sadollahkhani, I. Kazeminezhad, J. Lu, O. Nur, L. Hultman, and M. Willander, "Synthesis, structural characterization and photocatalytic application of ZnO@ZnS core-shell nanoparticles," *RSC Adv.*, vol. 4, no. 70, pp. 36940–36950, 2014.
[20] M. Azimi, M. S. Sadjadi, and N. Farhadyar, "Fabrication and characterization of core/shell ZnO/gold nanostructures and study of

their structural and optical properties," *Orient. J. Chem.*, vol. 32, no. 5, pp. 2517–2523, 2016.

[21] A. A. Ismail, A. V. Gholap, and Y. A. Abbo, "Enhancement of local electric field in core-shell orientation of ellipsoidal metal/dielectric nanoparticles," *Condens. Matter Phys.*, vol. 20, no. 2, pp. 1–11, 2017.

[22] H. Kettunen, H. Wallén, and A. Sihvola, "Electrostatic resonances of a negative-permittivity hemisphere," *J. Appl. Phys.*, vol. 103, no. 9, 2008.

[23] S. E. Starodubtcev, N. V. Korolev, A. F. Klinskikh, and P. A. Meleshenko, "Reduced polarizability and local-field effect in self-assembled ensemble of nanoparticles," *J. Nano- Electron. Phys.*, vol. 5, no. 1, pp. 1–5, 2013.

[24] U. K. Chettiar and N. Engheta, "Internal homogenization: Effective permittivity of a coated sphere," *Opt. Express*, vol. 20, no. 21, p. 22976, 2012.

[25] A. Derkachova, K. Kolwas, and I. Demchenko, "Dielectric Function for Gold in Plasmonics Applications: Size Dependence of Plasmon Resonance Frequencies and Damping Rates for Nanospheres," *Plasmonics*, vol. 11, no. 3, pp. 941–951, 2016.

[26] L. J. Mendoza Herrera, D. M. Arboleda, D. C. Schinca, and L. B. Scaffardi, "Determination of plasma frequency, damping constant, and size distribution from the complex dielectric function of noble metal nanoparticles," *J. Appl. Phys.*, vol. 116, no. 23, 2014.

[27] S. Link and M. A. El-sayed, "Shape and size dependence of radiative, non-radiative and photothermal properties of gold nanocrystals," *Int . Re v i e w s i n Ph y s i c a l Ch e m i s t r yt*, vol. 19, no. 3, pp. 409–453, 2000.

[28] W. Lv, P. E. Phelan, R. Swaminathan, T. P. Otanicar, and R. A. Taylor, "Multifunctional Core-Shell Nanoparticle Suspensions for Efficient Absorption," *J. Sol. Energy Eng.*, vol. 135, no. 2, p. 021004, 2012.

[29] L. Jule, V. Mal'nev, B. Mesfin, T. Senbeta, F. Dejene, and K. Rorro, "Fano-like resonance and scattering in dielectric(core)-metal(shell) composites embedded in active host matrices," *Phys. Status Solidi Basic Res.*, vol. 252, no. 12, pp. 2707–2713, 2015.

[30] N. Daneshfar and K. Bazyari, "Optical and spectral tunability of multilayer spherical and cylindrical nanoshells," *Appl. Phys. A Mater. Sci. Process.*, vol. 116, no. 2, pp. 611–620, 2014.

[31] A. R. Bijanzadeh, "A study of the surface plasmon absorption band for nanoparticles," *Int. J. Phys. Sci.*, vol. 7, no. 13, pp. 1943–1948, 2012.

[32] L. T. Jule *et al.*, "Wide visible emission and narrowing band gap in Cd-doped ZnO nanopowders synthesized via sol-gel route," *J. Alloys Compd.*, vol. 687, no. July, pp. 920–926, 2016.

[33] S. C. Singh, R. K. Swarnkar, and R. Gopal, "Zn/ZnO core/shell nanoparticles synthesized by la ser ablation in aqueous environment: Optical and structural characterizations," *Bull. Mater. Sci.*, vol. 33, no. 1, pp. 21–26, 2010.

[34] A. Sambou, B. D. Ngom, L. Gomis, and A. C. Beye, "Turnability of the Plasmonic Response of the Gold Nanoparticles in Infrared Region," *Am. J. Nanomater.*, vol. 4, no. 3, pp. 63–69, 2016.